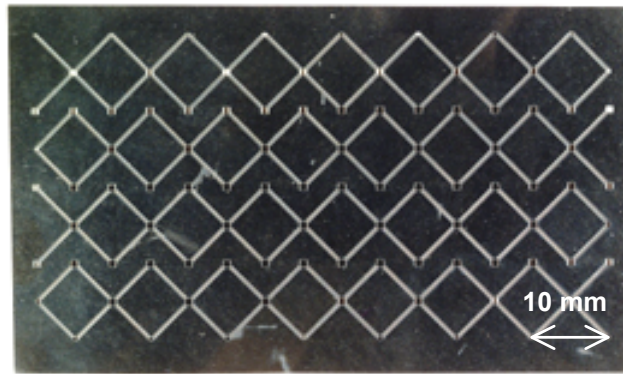


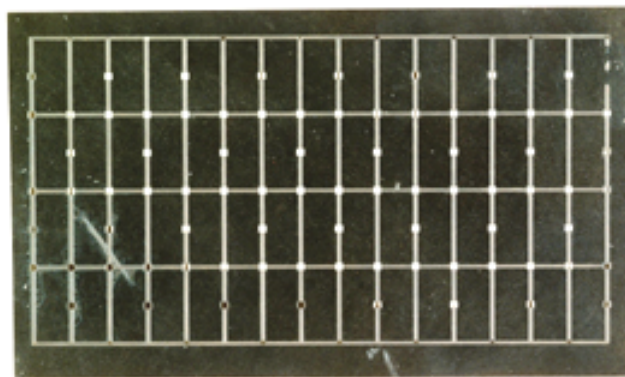
Figure 6.17 Optical microphotographs of the Ti-rich TiNi SMA sheet etched with the etchant ratio of HF:HNO₃:H₂O=1:1:4.

Figures 6.18(a) and (b) show the photographs of the entire back and front of the Ti-rich TiNi SMA sheet etched using the ratio of HF:HNO₃:H₂O = 1:1:4. Good folding patterns were produced uniformly across the entire area of the sheet. Figures 6.19(a) and (b) show close-up photographs of the same sheet. Interestingly, the square holes made by double sided etching are clear through the sheet, a distance of 0.08 mm or 0.04 mm on each side, even though the average etched depth of the single-sided lines was a slightly shallower 0.0365 mm.

An SEM examination focused on the area of the sheet that is specified in Figure 6.20(a). Figures 6.20(b) and (c) show photomicrographs of the top (location A) and side (location B) views of the etched surface of the Ti-rich TiNi SMA sheet magnified at x130 and x150 times, respectively. The etched surface is smooth (relatively unpitted), which is a successful result, indicating that etching does not adversely affect the surface of the SMA sheet.

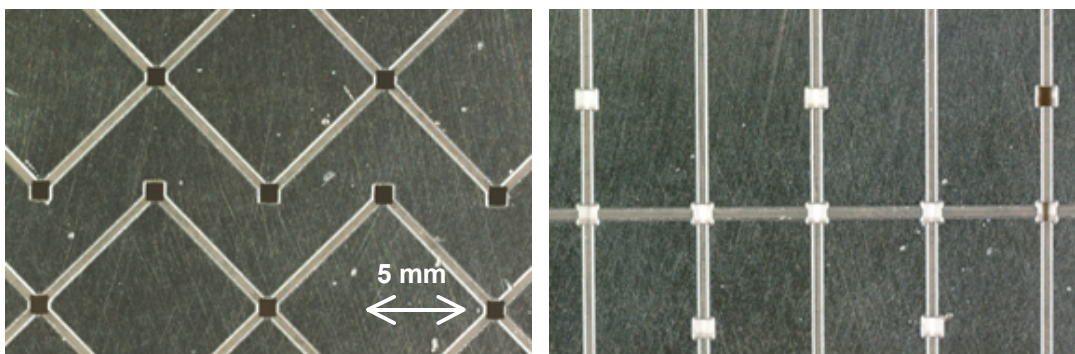


(a)



(b)

Figure 6.18 Photographs of the etched pattern into (a) back and (b) front side of the Ti-rich TiNi SMA sheet.



(a)

(b)

Figure 6.19 Close up photographs of the etched pattern into (a) back and (b) front side of the Ti-rich TiNi SMA sheet.

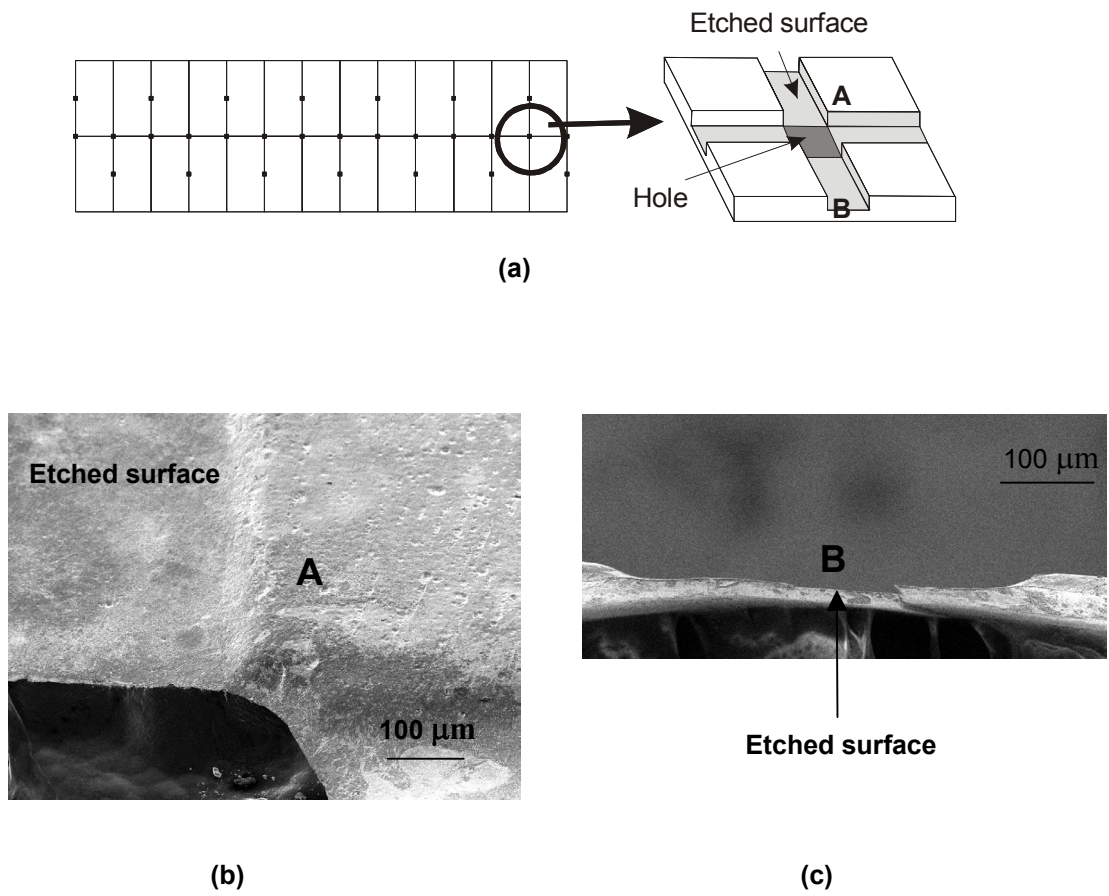


Figure 6.20 (a) Illustration showing the locations of the SEM observation (b) Projection and (c) side view of photomicrographs of the etched Ti-rich TiNi SMA sheet.

6.3.3 Negative etching

During the negative etching process a single dry photoresist of 0.035 mm in thickness peeled off immediately after etching started. It was not resistant enough to adhere to the SMA sheet. However, the etching pattern was successfully transferred onto the sheet when a double layer of photoresist totaling 0.070 mm in thickness was used. The error from the original width in the artwork was below 0.05%, implying that the exposure time was correct. Cracking of the photoresist did not occur, indicating that the baking temperature and time were also correct.

A sheet with the dry photoresist was etched with the etchant ratio of HF:HNO₃:H₂O = 1:1:4. Figures 6.21, 6.22 and 6.23 show the results of etched depth, undercut and etch factor with respect to the etch time. In these figures, filled symbols are the results of negative etching, and for comparison, the results of positive etching using the same etchant are also shown. Etch speed is almost the same as that with the positive liquid photoresist. However, the undercut is smaller. Therefore, the etch factor is larger for negative etching (between 0.3 and 0.5) than for positive etching.

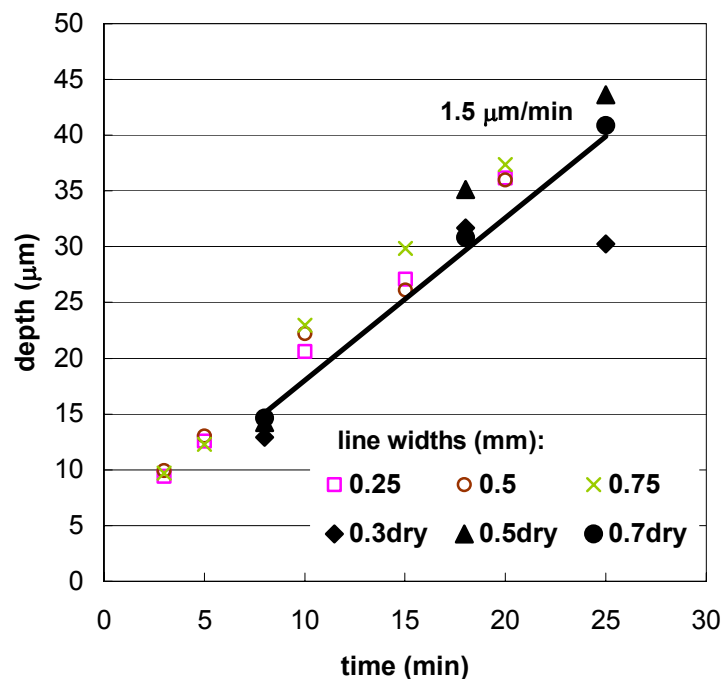


Figure 6.21 Change of etch depth with time for negative etching of SMA sheet.

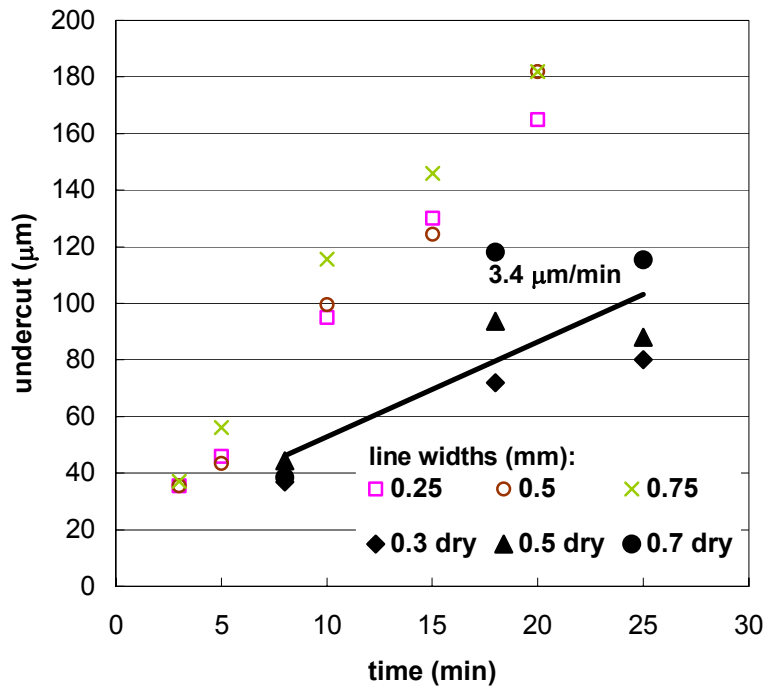


Figure 6.22 Change of undercut with time for negative etching of SMA sheet.

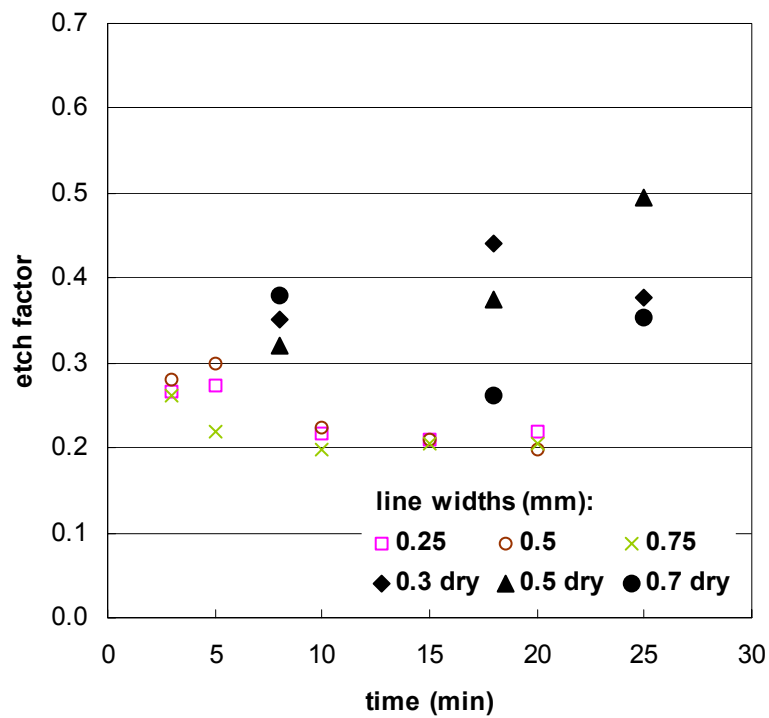


Figure 6.23 Etching factor with time for negative etching of SMA sheet.

6.3.4 Factors influencing etching process

- **Etchant ratio of HF/HNO₃**

The positive etching experiment revealed that a ratio of HF:HNO₃:H₂O = 1:4:5 is not suitable to etch SMA sheet. The ratio of HF and HNO₃ was too high, causing the photoresist to peel off during etching.

When the etchant ratio of HF:HNO₃:H₂O = 1:1:2 was used, the etch speed was 3.2 μm/min, which is twice as fast as the etch speed when the etchant ratio of HF:HNO₃:H₂O = 1:1:4 was used. However, as shown in Figures 6.12(b) and 6.16(b), the etchant of HF:HNO₃:H₂O = 1:1:2 had adverse affects on the sheet. Therefore a conclusion of this test is that an etchant ratio of 1:1:4 is the most suitable for a clean, undamaged etched surface. It may be possible however to improve etching speed (and production costs) by using a higher ratio of HF/HNO₃ etchant at the beginning of the etching process, and then switching to a more diluted mixture.

- **Photoresists**

Both positive and negative photoresists can be used for etching of SMA sheets. The experiments showed that the positive photoresist is tougher and adheres to the sheet better. A positive photoresist with a thickness of only 0.006 mm gave reliable results, whereas a negative photoresist with a much higher thickness of 0.035 mm peeled off during etching. A double-coated negative photoresist was able to withstand the etching process. The advantage of the thin photoresist is that it can allow a much finer etching resolution. Therefore, a positive photoresist would be a more useful technique when focus is directed towards the miniaturisation of the stent or stent graft for coronary use. The advantages of negative etching are that the etching process is easier and cheaper. Furthermore, uniform coating can be applied over a large area, which would become particularly important in the large scale manufacture of stents and stent grafts.

From the results of the negative etching given in Figure 6.21, it is found that etching speed was the same as that of the positive etching. However, from Figure 6.23, the undercut for the negative etching is smaller than that of the positive etching, which is because of thicker photoresist. Using the negative photoresist, etch factors were improved from 0.25 to between 0.3 and 0.5 when the etchant of HF:HNO₃:H₂O was diluted to 1:1:4. However, this is still a very small etch factor compared with that for the other materials, such as, stainless steel or copper (1.5–2.0), because SMA has poor etching characteristics (Allen 1986). The small etch factor indicates that the etched slope is not sharp, which might be a rather good property for the stent design because it can alleviate concentrations of stress when the sheet is folded.

- **Etched width and the double sided etching**

In the case of HF:HNO₃:H₂O = 1:1:4, as shown in Figures 6.14, the etching speed become faster when the width is larger than 0.75 mm. As shown in Figure 6.13(a), the undercut also increases when the etched groove width is greater than 0.75 mm. These are the results of the one sided etching. When double side etching is carried out, the values of the undercut of lines and the square holes of 0.3 and 0.8 mm in width were the same, as shown in Figure 6.20. Because in general, the undercut with double sided etching is smaller than that with one sided etching (also shown by Allen 1986), the undercut of square holes is not excessive. In order to get the desired depth and widths for the stent folding patterns, the etched depth and size of undercut for single or double sided etching should be taken into account during the design stage.

6.3.5 Bending test

Figure 6.24 shows the results of the bending test. The specimens have an etched groove width w_g of 0.7 mm and have cuts in different directions with respect to the rolling direction. For 0° , the specimen fails through cracking. For 45° , ε is 2.4% and the recovery rate is 95.8%, i.e., the specimen recovers almost to the original flat shape. However, the specimen is cracked when ε is larger than 2.4%. For 90° , ε is 2.4% and the recovery rate is 92.5%, i.e., the specimen also recovered almost to the original flat shape. At this angle to the rolling direction the specimen could be bent until ε is 8.9%.

Table 6.2 shows the recovery ratios with different w_g and angle. When w_g was 0.3 mm, all of the specimens cracked. For 0° , all specimens also cracked. For 45° or 90° , the specimen with w_g equal to 0.5 or 0.7 mm and ε is less than 3%, the specimens recovered almost completely to their original flat shapes when heated.

These results show that the direction of the cut with respect to the rolling direction of the Ti-rich TiNi SMA sheet is important. It is best to make cuts at 90° , and acceptable to make cuts at 45° , but it is not recommended to make the cuts at 0° to the rolling direction. Furthermore, the width of the cut is important, and gives a better result if it is greater than 0.5 mm.

Table 6.2 Recovery ratio (%) of effects of etched grooves width and direction.

w_g	Recovery ratio (%)								
	0.3 (mm)			0.5 (mm)			0.7 (mm)		
strain (%) (deg)	less than 3	3-6	more than 6	less than 3	3-6	more than 6	less than 3	3-6	more than 6
0	C	C	C	C	C	C	C	C	C
45	C	C	C	96.10	C	C	95.77	C	C
90	C	C	C	92.12	87.69	C	92.50	82.27	71.83

C:crack when the specimen was bent

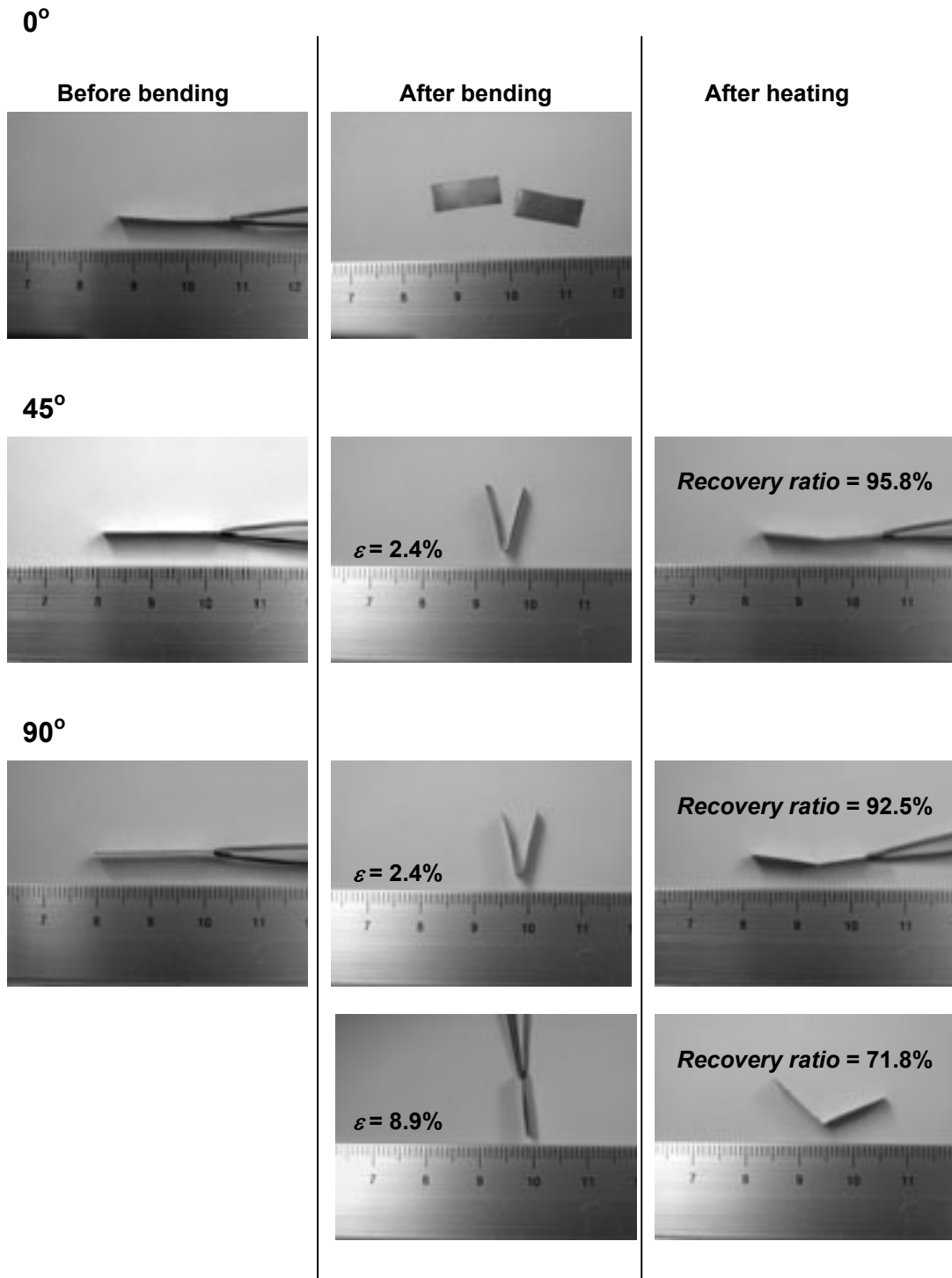


Figure 6.24 Photographs of the specimen of $w_g = 0.7$ mm with angles between cuts and the rolling direction being 0° , 45° and 90° .

6.3.6 Heat treatment

Figure 6.25(a) shows the DSC profile of the Ti-rich TiNi SMA before annealing. The SMA exhibited an R phase⁴ transformation peak only when the SMA was cooling. The starting and finishing temperatures of R phase martensite crystal structure R_s and R_f were 334.9K and 315.7K, respectively. Then, when the SMA was heated, the starting and finishing temperatures of austenite crystal structure A_s and A_f were 318K and 344.8K, respectively. Figure 6.25(b) and (c) show the DSC profile of the SMA sheet annealed at 773K, and 1073K, respectively. In both cases, the transformation temperatures were similar. The temperatures of starting and finishing of martensite M_s and M_f were about 342K and 330K, respectively during cooling. A_s and A_f were 363K and 377K, respectively, during heating. It is found that the annealing process causes the transformation temperatures to rise by 10 to 20K, but they do not depend on the annealing temperature or the annealing time.

Figure 6.26 shows the results of recovery ratios with respect to the strain for the SMA sheet with and without annealing. Two things are found here. Firstly, the ductility of the SMA sheet is improved by annealing. The maximum surface strain of the specimen before annealing is 4.49%. After annealing at 773K and 1073K, it becomes 6.85% and 5.76%, respectively. Secondly, the shape memory effect is decreased by annealing. The recovery ratio of the specimen without annealing is 100%. The recovery ratio becomes less than 80% and 60% when the specimens are annealed at 773K and 1073K, respectively. Annealing at 1073K eliminated most of the dislocations in the materials, thus a permanent plastic deformation was introduced by the bending tests, leading to a poor shape recovery. Annealing at 773K resulted in an only partial elimination of dislocations, which gave an adequate deformability to the materials. As a result, the specimen annealed at 773K showed better shape recovery than that in the

⁴ R phase represents a trigonal crystal structure of martensite phase (Otsuka, et. al 1998).

specimen annealed at 1073K. Therefore it is better to anneal the SMA sheet at 773K for 10 minutes.

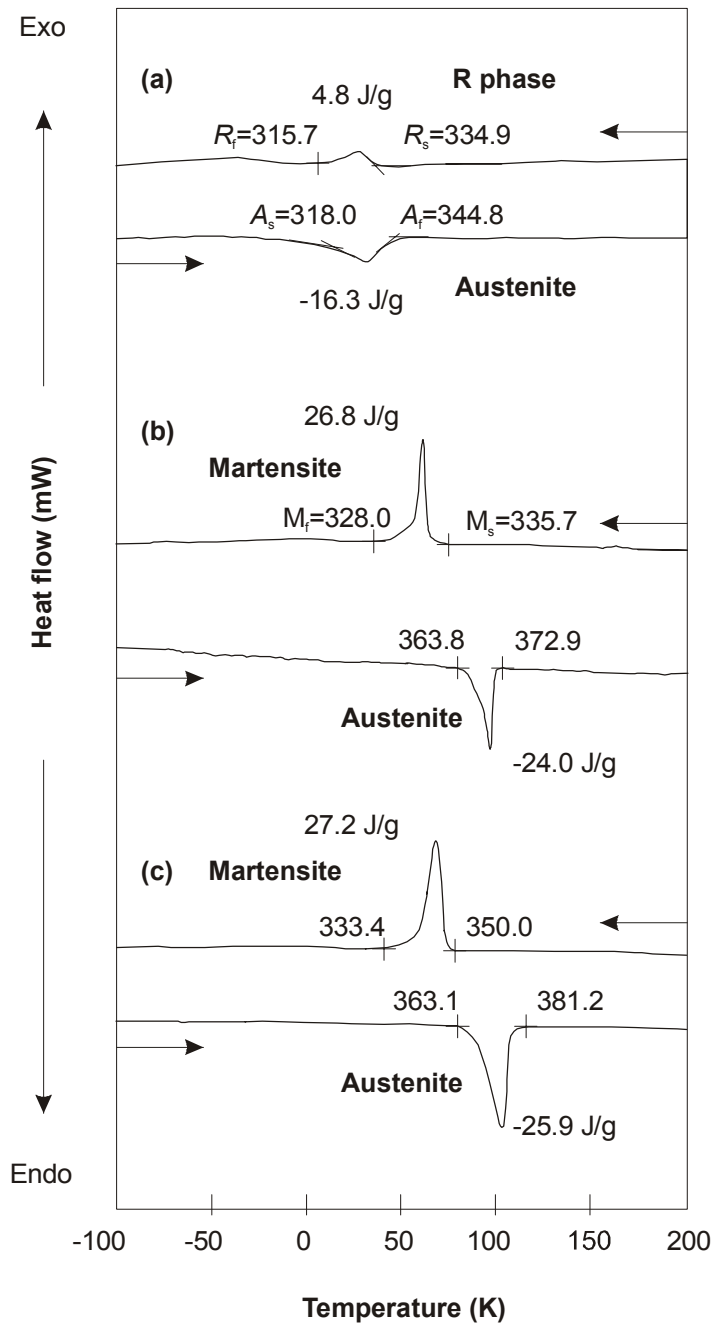


Figure 6.25 DSC profiles of Ti-rich TiNi SMA (a) before annealing, (b) annealed at 773K and (c) annealed at 1073K.

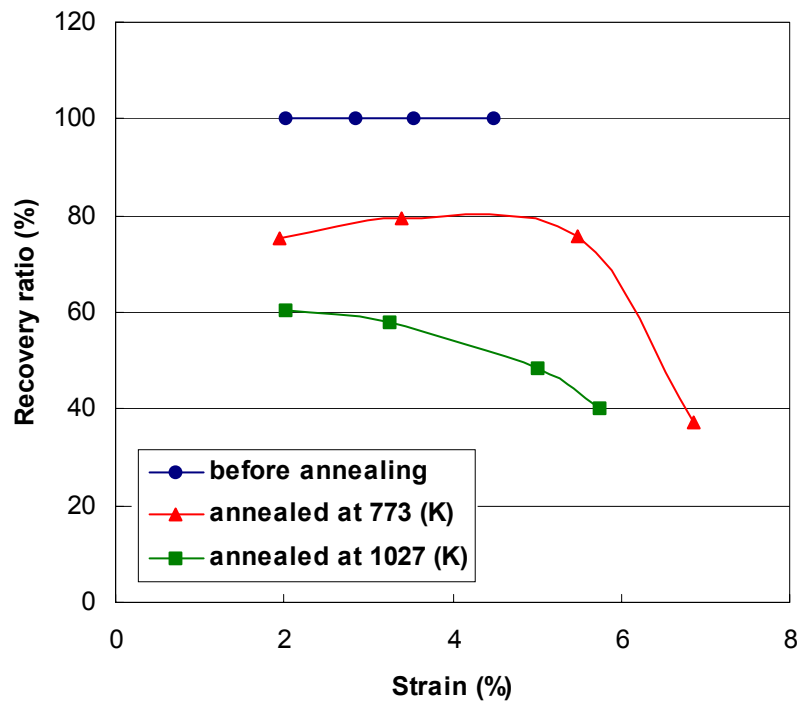


Figure 6.26 Recovery ratio vs. strain of the Ti-rich TiNi SMA with and without annealing.

6.4 Ti-rich TiNi shape memory alloy origami stent graft

In the previous sections, the pattern of the folds for the novel origami stent graft has been successfully etched into the Ti-rich TiNi SMA sheet, see Figures 6.18 and 6.19. Using the same sheet, the stent graft is produced. We now examine whether it can be self-deployed when heated.

Consider the shape the Ti-rich SMA sheet. Its initial shape is flat. Therefore, it always reverts back to a flat shape when heated. However, to produce the stent graft it must be a cylindrical shape in its fully expanded configuration. The SMA sheet was therefore annealed to store the memory of the cylindrical shape. This annealing process was carried out at the same time as doing heat treatment for improving ductility of the SMA described in the previous section. The etched SMA sheet was constrained to a cylindrical shape by an aluminum tube and heat-treated at 773K for 10 minutes. After the annealing process the stent graft was then folded at room temperature. It was heated at 383K and its self-deployment was recorded using a digital video camera.

The result of the shape of Ti-rich TiNi SMA sheet after heat treatment is shown in Figure 6.27. The sheet becomes a cylindrical tube, as expected and designed. The opposite edges of the sheet were then connected by adhesive. The radius and length of the origami stent graft is 12.7 and 40 mm, respectively. The radius is the same size as the existing oesophageal and aortal stent grafts.

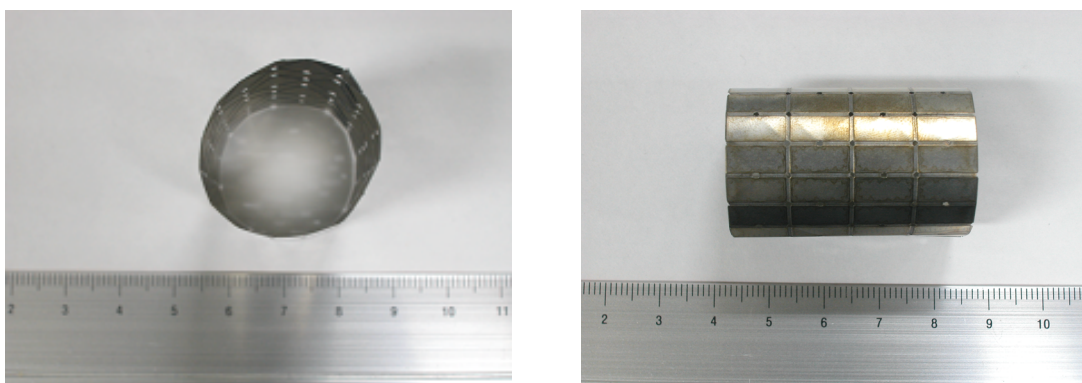


Figure 6.27 Ti-rich TiNi SMA tube produced by annealed at 737K.